JACS
JOURNAL OF THE AMERICAN CHEMICAL SOCIETY

ARTICLE

pubs.acs.org/JACS

Millisecond Dynamics in Glutaredoxin during Catalytic Turnover Is Dependent on Substrate Binding and Absent in the Resting States

Kristine Steen Jensen,† Jakob R. Winther, and Kaare Teilum*

Department of Biology, University of Copenhagen, Ole Maaløes Vej 5, 2200 Copenhagen N, Denmark

Supporting Information

ABSTRACT: Conformational dynamics is important for enzyme function. Which motions of enzymes determine catalytic efficiency and whether the same motions are important for all enzymes, however, are not well understood. Here we address conformational dynamics in glutaredoxin during catalytic turnover with a combination of NMR magnetization transfer, R_2 relaxation dispersion, and ligand titration experiments. Glutaredoxins catalyze a glutathione exchange reaction, forming a stable glutathinoylated enzyme intermediate. The equilibrium between the reduced state and the glutathionylated state was biochemically tuned to exchange on the millisecond time scale. The conformational changes of the protein backbone during catalysis were followed by ^{15}N nuclear spin relaxation dispersion experiments. A conformational transition that is well described by a two-state process with an exchange rate corresponding to the glutathione exchange rate was observed for 23 residues. Binding of reduced glutathione resulted in competitive inhibition of the reduced enzyme having kinetics similar to that of the reaction. This observation couples the motions observed during catalysis directly to substrate binding. Backbone motions on the time scale of catalytic turnover were not observed for the enzyme in the resting states, implying that alternative conformers do not accumulate to significant concentrations. These results infer that the turnover rate in glutaredoxin is governed by formation of a productive enzyme−substrate encounter complex, and that catalysis proceeds by an induced fit mechanism rather than by conformer selection driven by intrinsic conformational dynamics.

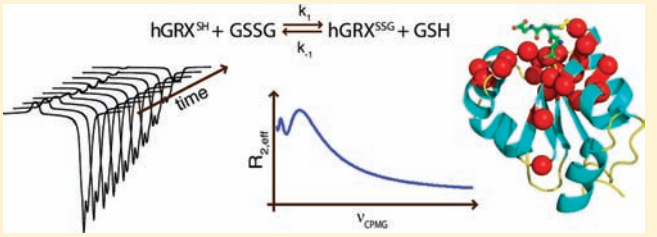

INTRODUCTION

The link between structure and function of enzymes has been investigated for decades, and significant insight has been gained in the coupling of static aspects to enzyme function. The connection between enzyme function and dynamics, by contrast, is only partially resolved. Proteins undergo fluctuations on different time scales, ranging from femtoseconds to picoseconds for vibrations, and up to hours for rearrangements of subunits and for folding of some proteins.[1] Particular attention has been paid to microsecond−millisecond conformational motions of enzymes since macroscopic turnover occurs on a similar time scale. This similarity suggests that these motions are the rate-limiting factor of enzyme catalysis.[2−4]

In purely thermodynamic terms, enzymes catalyze reactions by decreasing the activation energy for formation of the transition state. The molecular mechanism underlying this ability is not fully understood, however. The lifetime of a typical enzyme transition state is gauged from ab initio transition-path sampling calculations on the order of femtoseconds.[5] Given this short lifetime and that the transition state should be regarded as highly dynamic, the much slower microsecond−millisecond conformational motions cannot directly influence the chemical reaction coordinate. Motions on these slower time scales can affect the reaction coordinate in other ways.[5] Conformational changes can facilitate access of the substrate to the catalytic site, control the correct conformation of the catalytic residues, and promote product release as exemplified by ribonuclease A.[6] Investigations of the effect of ligand binding on conformational fluctuations in dihydrofolate reductase have revealed a dependency on ligand type.[7] Fluctuations in the substrate loop are present only when substrates are bound to the enzyme but not when cofactors or products are bound. The observed motions do not correlate with substrate or cofactor association or dissociation from the enzyme.[8] These findings indicate that microsecond−millisecond dynamic motions in some enzymes may function by directional steering of catalysis through conformer selection.[7]

Determining microsecond−millisecond motions during catalytic turnover results in a more complete description of the enzymatic energy landscape. NMR relaxation dispersion techniques offer unique possibilities to study exchange processes on the microsecond−millisecond time scale of proteins in solution at atomic resolution.[9,10] This requires that the exchange rate between magnetically different states is within the time-window of the experiments. Minor populated states exchanging with higher populated states are then probable. For many enzymes this is not achievable since the equilibrium is shifted far toward product formation and the reactions, therefore, in practical terms are irreversible. The dynamics of two types of enzymes, prolyl cis−trans isomerases and adenylate kinases, however, have been

Received: October 27, 2010
Published: February 16, 2011

dx.doi.org/10.1021/ja1096539 | J. Am. Chem. Soc. 2011, 133, 3034–3042

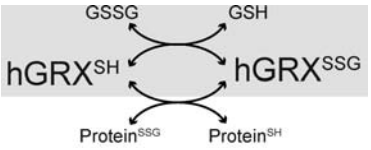

Figure 1. Catalytic cycle of glutaredoxin. The reversible reaction of protein cysteinyl glutathionylation is catalyzed by glutaredoxin (hGRX). The reaction takes place through two successive thiol−disulfide exchange reactions with a stable glutathionylated enzyme intermediate ($hGRX^{SSG}$). The shaded box encloses the part of the reaction cycle studied in the present work, in which glutaredoxin catalyzes the glutathione interchange.

investigated during catalysis.[2,11−15] The results revealed a correlation between catalytic turnover and conformational fluctuations. The frequencies of movements during catalysis occurred also in the resting enzymes, and both types of enzymes followed conformational selection where on-pathway conformers were sampled in the substrate-free state and in the product-bound state.[10,11]

The rate of ligand binding may in general also be limited by conformational changes induced by bound ligand (induced fit) or by diffusion as inferred by the flexible protein recognition model.[16] The induced fit mechanism of substrate binding lacks a kinetic description of the rate-limiting step.[17] Nevertheless, discrimination of induced fit from conformer selection requires kinetic data since the observation of structural change between ligand-free and ligand-bound enzyme does not tell if the conformational change occurred before or after binding of ligand. The two mechanisms may also be combined where conformer selection is followed by a ligand -induced structural change.[16,18,19]

We have investigated motions on the microsecond−millisecond time scale of human glutaredoxin 1 (hGRX) during catalysis and in the resting states. hGRX is an oxidoreductase localized to the cytosol. It has five cysteine residues of which two are present in the active site, in a CPYC motif. Other glutaredoxins that have a CPYX motif exist.[20] The N-proximal cysteine (Cys23) is the catalytic residue, forming a disulfide bond to glutathione during the reaction. $hGRX^{4CS}$ is a variant of the enzyme in which the four noncatalytic cysteine residues are replaced by serine. Potential glutathionylation of other sites in the enzyme is thereby prevented. This variant has the same efficiency as the wild type enzyme in catalysis of deglutathionylation of glutathionyl mixed disulfides.[21] The active site cysteine has a very low pK_a (3.5) ensuring nearly complete deprotonation of Cys23 at pH 7.[22] Because the concentration of the Cys23 anion is high, Cys23 becomes a good leaving group, optimized for thiol−disulfide exchange.[23] In the reversible reaction of protein glutathionylation, a stable glutathionylated enzyme intermediate is formed (Figure 1). This allows studies of the reaction with glutathione as the sole substrate. Combined these properties provide a unique opportunity for studying conformational dynamics during catalytic turnover in an enzyme under equilibrium conditions. The ratio of glutathionylated to reduced $hGRX^{4CS}$ is tunable by changing the ratio of reduced glutathione (GSH) to oxidized glutathione (GSSG). The exchange rate between reduced and glutathionylated $hGRX^{4CS}$ is tunable by varying the total glutathione concentrations.

We show that $hGRX^{4CS}$ does not exhibit microsecond−millisecond conformational changes in the resting states. Motions are detectable during the reaction and when an off-pathway complex of the reduced enzyme with GSH is formed. These observations indicate that the microsecond−millisecond motions in $hGRX^{4CS}$ result from substrate binding and not from crossing of the transition state energy barrier of product formation. Instead substrate binding induces a conformational change.

EXPERIMENTAL SECTION

Expression and Purification. A plasmid with cDNA encoding $hGRX^{4CS}$ in pET24a(+) (synthesized by GenScript) was used for expression in *E. coli* BL21(DE3) Rosetta. All cell growth was at 37 °C. For production of unlabeled $hGRX^{4CS}$, cultures were grown in LB medium and protein expression was induced with IPTG (0.5 mM) at OD_{600} = 0.8. Cultures were left for 5 h before harvest. For uniformly ^{15}N labeled and $^{13}C,^{15}N$ labeled $hGRX^{4CS}$, cultures were first grown in LB medium to OD_{600} = 0.8. Then cells were harvested and resuspended in M9 minimal medium containing 1 g/L $^{15}NH_4Cl$ and 4 g/L glucose ($[U-^{13}C_6]$-glucose) as the sole nitrogen and carbon sources and grown for 1 h before induction with IPTG. Cells were harvested 4−5 h after induction. $hGRX^{4CS}$ was purified essentially as described in ref 21 with the addition of a final RP-HPLC step. For this step, $hGRX^{4CS}$ was reduced by incubation with DTT (10 mM) for 1 h at room temperature. TFA was added to the reduced sample to a concentration of 0.5%, and the sample was eluted from a Zorbax C18 semipreparative column by a gradient from 30% acetonitrile in 0.1% TFA to 70% acetonitrile in 0.05% TFA. Fractions containing $hGRX^{4CS}$ were flash frozen in liquid nitrogen and lyophilized. The identity and degree of labeling of $hGRX^{4CS}$ was confirmed by MALDI-MS. Concentrations of $hGRX^{4CS}$ were determined using a calculated extinction coefficient at 280 nm of 2980 $M^{-1}cm^{-1}$.

Glutathione Concentration Determinations. Samples of 50 μL were mixed with 50 μL of 1 M HCl and analyzed by RP-HPLC on a C18 RP-column (Pep-mass) using 0.05% TFA and a linear gradient from 0 to 50% acetonitrile. Absorption was detected at 248 nm. Standard curves for reduced glutathione (GSH) and oxidized glutathione (GSSG) were made to link peak areas with concentration. For this purpose the concentration of a GSH stock was determined in triplicate by reaction with DTNB (ε_{TNB} = 14150 M^{-1} cm^{-1}), and the GSSG concentration was determined in triplicate from the absorbance (ε_{248} = 382 M^{-1} cm^{-1}).

NMR. All NMR samples were in 10 mM Na-phosphate pH 7.0, 1 mM 4,4-dimethyl-4-silapentane-1-sulfonic acid, and 10% D_2O, and all NMR experiments were performed at 25 °C. NMR relaxation experiments were performed on a Varian Inova 750 MHz spectrometer with a triple-resonance probe. Assignments and titration experiments were performed on a Varian Inova 800 MHz spectrometer with a triple-resonance cryoprobe. One-dimensional ^1H spectra were transformed and analyzed in VnmrJ 2.2D. Multidimensional spectra were processed in nmrPipe[24] and analyzed with nmrPipe and CcpNmr Analysis. Peak intensities in $^1H,^{15}N$-HSQC spectra were determined by summing the intensities in a 3 × 3 points window centered at the peak maximum.

Assignment of $hGRX^{4CS}$. Backbone resonances of reduced $hGRX^{4CS}$ were assigned using $^1H-^{15}N$ HSQC, HNCA, and HNCACB experiments and the published assignment of reduced wild type hGRX.[25] The sample was 1 mM $hGRX^{4CS}$ with 5 mM DTT. The assignment of backbone resonances of glutathionylated $hGRX^{4CS}$ could be transferred from published assignments[21] using an HNCA. Glutathionylated glutaredoxin was prepared by incubation of reduced glutaredoxin with an excess of GSSG (100 mM) at room temperature for 2 h. Excess glutathione was removed by dialysis (MWCO 3500). The protein concentration in the final sample was 1 mM.

GSH binding to reduced $hGRX^{4CS}$ was measured by titration of $^{13}C,^{15}N$- $hGRX^{4CS}$ with GSH in the presence of 5 mM DTT. GSH was added directly to the NMR tube from a concentrated stock, and the sample was purged with argon after each addition. For each

dx.doi.org/10.1021/ja1096539 |*J. Am. Chem. Soc.* 2011, 133, 3034–3042

concentration of GSH a ^{15}N-HSQC was recorded. The GSH and glutaredoxin concentrations after each titration were calculated, accounting for the volume increase. The change in chemical shift was calculated as the weighted sum of the ^{1}H and ^{15}N chemical shifts relative to the chemical shifts of free reduced hGRX^{4CS} $\Delta\delta = ((\delta^{1}H_{[GSH]} - \delta^{1}H_{[GSH]=0})^2 + (0.15(\delta^{15}N_{[GSH]} - \delta^{15}N_{[GSH]=0}))^2)^{1/2}$. Data were fitted to eq 1:

$$\Delta\delta = \frac{\Delta\delta_{max}[GSH]}{K_2^{-1} + [GSH]} \quad (1)$$

$\Delta\delta_{max}$ is the change in chemical shift upon saturation and K_2^{-1} is the dissociation constant for GSH.

Magnetization Transfer Analysis of hGRX Catalysis. The turnover of GSSG to GSH was followed in experiments with hGRX^{4CS} concentrations of 15, 25, 50, and 100 μM. [GSSG] was kept at 1 mM while [GSH] was varied (5, 10, 20, and 30 mM). Experiments with 10 mM GSSG and 50 mM GSH were conducted to verify the proposed model. The exact concentrations of GSSG and GSH in the samples after equilibration with hGRX^{4CS}, and both before and after the NMR experiment, were determined as described above. The magnetization of H$^{\beta1}$ in GSSG was selectively inverted relative to the H$^{\beta1}$ of GSH, and the change in longitudinal magnetization of GSSG H$^{\beta1}$ was measured in a series of one-dimensional ^{1}H spectra. The pulse sequence by Robinson et al.[26] with a watergate added was used with relaxation delays (τ) from 0.01 ms to 2 s. The phase cycling was chosen so peak areas go toward zero at complete relaxation. The peak area, I, of the GSSG specific peak as function of the relaxation delay was fitted to a biexponential function:

$$I(\tau) = A\, e^{-\lambda_1\tau} + B\, e^{-\lambda_2\tau} \quad (2)$$

For analyzing the magnetization transfer data, both the reaction between GSSG and hGRX^{SH} and GSH and hGRX^{SH} were considered as shown in Schemes 1 and 2:

$$hGRX^{SH} + GSSG \underset{k_{-1}}{\overset{k_1}{\rightleftarrows}} hGRX^{SSG} + GSH \quad \text{(Scheme 1)}$$

$$hGRX^{SH} + GSH \underset{k_{-2}}{\overset{k_2}{\rightleftarrows}} hGRX^{SH}\cdot GSH \quad \text{(Scheme 2)}$$

The sum of the eigenvalues ($\lambda_1 + \lambda_2$) in eq 2 is equal to the sum of the exchange rate between reduced and oxidized glutathione (k'_{ex}) and the average longitudinal relaxation rate for all glutathione species $R_1^{glutathione}$:

$$\lambda_1 + \lambda_2 = k'_{ex} + R_1^{glutathione} \quad (3)$$

where k'_{ex} is given by

$$k'_{ex} = k_1[hGRX^{SH}] + k_{-1}[hGRX^{SSG}] \quad (4)$$

The individual concentrations of hGRX^{SH} and hGRX^{SSG} in the reaction mixture are too low for accurate determination. Therefore k'_{ex} should be expressed as a function of the total enzyme concentration:

$$c_{total}^{hGRX} = [hGRX^{SH}] + [hGRX^{SSG}] + [hGRX^{SH}\cdot GSH] \quad (5)$$

Rearranging the equilibrium constants K_1 and K_2 corresponding to Schemes 1 and 2, respectively, gives

$$[hGRX^{SSG}] = \frac{K_1}{Q}[hGRX^{SH}] \quad (6)$$

$$[hGRX^{SH}\cdot GSH] = K_2[GSH][hGRX^{SH}] \quad (7)$$

where $Q = [GSH]/[GSSG]$. Substituting these two expressions into eq 5 yields the following expression for the concentration of reduced glutaredoxin:

$$[hGRX^{SH}] = \frac{c_{total}^{hGRX}}{1 + \frac{K_1}{Q} + K_2[GSH]} \quad (8)$$

Inserting eq 8 into eq 4 and using $k_{-1} = k_1/K_1$ yields

$$k'_{ex} = k_1 c_{total}^{hGRX}\left(\frac{1+Q}{Q + K_1 + K_2Q[GSH]}\right) \quad (9)$$

Finally, eq 9 may be inserted into eq 3 to give the following relation between the measured rates in the magnetization transfer experiment (λ_1 and λ_2) and the concentrations of hGRX and glutathione:

$$\lambda_1 + \lambda_2 = k_1 c_{total}^{Grx}\left(\frac{1+Q}{Q + K_1 + K_2Q[GSH]}\right) + R_1^{glutathione} \quad (10)$$

K_1 and k_1 were obtained by fitting eq 10 to the experimental data and setting K_2 to the value obtained in the GSH binding experiment.

^{15}N CPMG Relaxation Dispersion. In the ^{15}N Carr−Purcell−Meiboom−Gill (CPMG) relaxation dispersion experiments the exchange rate is determined by the glutathione concentrations:

$$k_{ex} = k_1[GSSG] + k_{-1}[GSH] \quad (11)$$

The [GSH]/[GSSG] ratio will control [hGRX^{SH}]/[hGRX^{SSG}] according to eq 6.

Three samples were studied: (i) hGRX^{4CS} actively catalyzing glutathione transfer was prepared by dialysis of a 1 mM ^{15}N-hGRX^{4CS} against a buffer containing 140 μM GSSG and 320 μM GSH. (ii) Reduced hGRX^{4CS} was prepared by mixing 1 mM ^{15}N-hGRX^{4CS} with 5 mM DTT. (iii) Glutathionylated hGRX^{4CS} was prepared by incubation of 1 mM reduced ^{15}N-hGRX^{4CS} with 100 mM GSSG and subsequently removing excess glutathione by RP-HPLC. ^{15}N CPMG relaxation-compensated experiments[27] were performed using the constant-time approach[28] with a relaxation delay of 60 ms. Relaxation dispersions were sampled using 12 CPMG field strengths (ν_{CPMG}) ranging from 50 to 1000 Hz. Data were fitted both to a constant and to the expression for a two-state process in slow exchange (eq 12).

$$R_{2,eff} = R_2 + k_a[1 - \mathrm{sinc}(\Delta\omega/4\nu_{CPMG})] \quad (12)$$

where R_2 is the transverse relaxation in the absence of exchange, k_a is the apparent pseudo-first-order rate constant for the forward (or reverse) reaction obtained by measuring $R_{2,eff}$ of the reduced (or oxidized) state, and $\Delta\omega$ is the chemical shift difference between the reduced and oxidized states.

The F-test was used to determine whether each residue showed significant dispersions with a significance criterion of $p < 0.05$, $R_{ex} = k_a(1 - \mathrm{sinc}(\Delta\omega/4\nu_{CPMG})) > 2\ s^{-1}$ and $k_a > \chi^2/2$.

$R_1\rho$ Relaxation Dispersion. A sample of 1 mM ^{15}N-hGRX^{4CS} with 1.7 mM GSH and 5 mM DTT was prepared. Relaxation series with six time delays (0, 0.02, 0.04, 0.06, 0.08, and 0.1 s) were recorded at spin-lock field strengths from 406 to 1212 Hz and with offsets ranging from −1000 to 10 000 Hz. The spin-lock field strengths were calibrated as described in ref 9. Each relaxation series was fitted to a monoexponential decay to obtain $R_1\rho$. The $R_1\rho$ rates were fitted to the expression for a two-state process in fast exchange (eq 13):

$$R_{1\rho} = R_1 \cos^2\theta + (R_2 + R_{ex})\sin^2\theta \quad (13)$$

where θ is the tilt angle, $R_{ex} = \Phi_{ex}k_{ex}/(k_{ex}^2 + \omega_{eff}^2)$, k_{ex} is the exchange rate between the two states, ω_{eff} is the effective field of the spin-lock, $\Phi_{ex} = \Delta\omega^2 p_A(1 - p_A)$, $\Delta\omega$ is the chemical shift difference between the exchanging states, and p_A is the relative population of one of the states. The F-test ($p < 0.01$) was used to determine if the R_{ex} contribution was significant by comparing fits to eq 13 where R_{ex} was either optimized or fixed at $R_{ex} = 0$.

Isothermal Titration Calorimetry. Reduced hGRX^{4CS} was titrated with GSSG at 25 °C on a MCS isothermal titration calorimeter (MicroCal LLC, Northampton, MA). Prior to the titration, hGRX^{4CS} was reduced by incubation with 100 mM DTT, 10 mM Na-phosphate, pH 7.0, for 2 h at room temperature followed by overnight incubation at 4 °C. DTT was removed by gel filtration on a PD-10 Sephadex-G25 column using argon-saturated 10 mM Na-phosphate, pH 7.0, as eluent. The fraction containing reduced glutaredoxin was concentrated by use of spin filters (MWCO 3000) to 165 μM. The GSSG stock of 1.60 mM was prepared in 10 mM Na-phosphate, pH 7.0. Glutaredoxin and GSSG stocks were thoroughly purged with argon and degassed by vacuum stirring for 20 min before hGRX^{4CS} was loaded into the ITC cell and GSSG was loaded in the syringe. Data were analyzed using an exchange model describing the reaction in Scheme 1 assuming that the measured change in enthalpy (ΔH) equals the change in standard enthalpy ($\Delta H°$).[29]

RESULTS

Characterization of the Glutaredoxin−Glutathione Equilibrium. To choose conditions that allow delineation of conformational fluctuations in hGRX^{4CS} during catalysis, the reaction needs to be characterized. This was accomplished using NMR magnetization transfer[30] at chemical equilibrium to determine the rate constants of the reaction between glutathione and glutaredoxin (Scheme 1). The relaxation rates comprise contributions from longitudinal relaxation and chemical exchange (Figure 2A and Scheme 1). A specific signal from one of the exchanging species is required, implying that the reaction has to be in slow exchange on the chemical shift time scale. The reaction was followed by measuring the change in magnetization of the H$^{\beta}$ resonance of the cysteinyl residue of glutathione, which splits upon formation of the disulfide bond present in GSSG.[31] An experiment series with varied enzyme concentrations and different GSH to GSSG ratios (Q) was conducted (Figure 2). High concentrations of GSH resulted in slower rates than expected from a single equilibrium between glutaredoxin and glutathione (Scheme 1) and thus made the apparent forward rate constant dependent on the GSH concentration. The simplest model to explain the observed behavior is that GSH may also bind to reduced hGRX^{4CS} and thereby decrease the effective enzyme concentration (Scheme 2).

To test this model, reduced hGRX^{4CS} was titrated with GSH, and ^{15}N−^{1}H amide chemical shifts changes were followed. Resonances experiencing a weighted chemical shift difference of at least 0.1 ppm were included in a global fit of the dissociation constant (Figure 3). All titrating resonances report on the same event and result in a dissociation constant of $K_2^{-1} = 15.4 \pm 0.3$ mM. A model containing the reactions of both Schemes 1 and 2 is thus necessary to describe the system (eq 10). Increasing the total concentration of glutathione ten times while keeping the ratio of GSH to GSSG near five did not result in deviation from the model. The equilibrium constants of the two reactions, K_1 and K_2, are strongly correlated in eq 10 and cannot be determined independently from fits of this equation to the experimental data. K_2 was fixed, therefore, to the value from the titration of reduced hGRX^{4CS} with GSH. Values of K_1, k_1, and the average longitudinal relaxation rate of glutathione $R_1^{glutathione}$ were optimized by fitting eq 10 to the kinetic data. The fit resulted in a forward rate constant k_1 of $(1.24 \pm 0.03) \times 10^6$ M^{-1} s^{-1}, an equilibrium constant K_1 of 29.1 ± 1.4, and a calculated backward rate constant k_{-1} of $(4.3 \pm 0.7) \times 10^4$ M^{-1} s^{-1}. K_1 was also

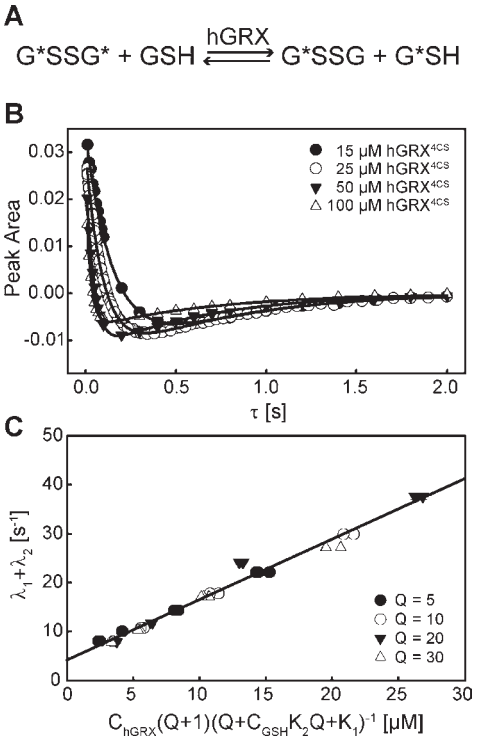

Figure 2. Determination of rate constants by magnetization transfer. (A) The rate constants are determined by observation of the glutaredoxin-catalyzed magnetization transfer between GSSG and GSH. Stars indicate the glutathione that originates in the oxidized state and emphasize the process of exchange between GSSG and GSH, which is catalyzed by hGRX. (B) Peak area of cysteinyl H$^{\beta}$ specific for GSSG (3.31 ppm) plotted as a function of the relaxation delay (τ) for $Q = 20$. Solid lines are fits to eq 2. The experiment was performed with 1 mM GSSG and 20 mM GSH at 25 °C, pH 7.0. (C) Data are plotted according to a model describing the glutaredoxin−glutathione equilibrium as the coupling of Schemes 1 and 2. X-axis values are calculated using the fitted value of K_1 and the value of K_2 obtained from the GSH titration. Error bars show standard errors from fits of eq 2 to the data. The straight line is drawn using eq 10 and the fitted values for k_1 ($(1.24 \pm 0.03) \times 10^6$ M^{-1} s^{-1}) and $R_{1,glutathione}$ (4.2 ± 0.3 s^{-1}).

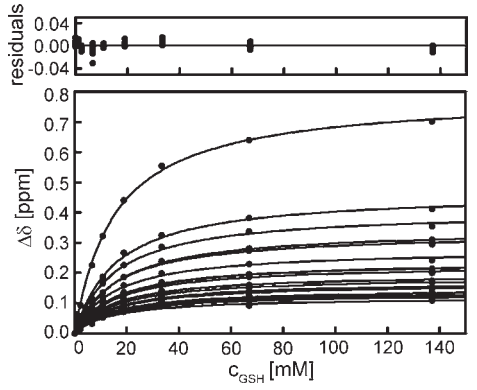

Figure 3. NMR titration of reduced hGRX^{4CS} with GSH. The experiment was conducted at 25 °C, Na-phosphate pH 7.0 with a 1 mM ^{13}C,^{15}N-hGRX^{4CS} sample. Changes in chemical shift were calculated as a weighted sum of the change in both direct and indirect dimension; $\Delta\delta = ((\delta^1H_{[GSH]} - \delta^1H_{[GSH]=0})^2 + (0.15(\delta^{15}N_{[GSH]} - \delta^{15}N_{[GSH]=0}))^2)^{1/2}$. The 23 resonances displaying a chemical shift difference larger than 0.1 ppm were included in a global fit to eq 1, which is represented by the solid lines.

dx.doi.org/10.1021/ja1096539 |J. Am. Chem. Soc. 2011, 133, 3034–3042

determined by isothermal titration calorimetry yielding an equilibrium constant of 35.1 ± 0.6, which is in good agreement with K_1 obtained from the NMR data. The analysis shows that three different states of $hGRX^{4CS}$ are populated at equilibrium, and that the enzyme cannot be saturated with either of the substrates at concentrations as high as 50 mM GSH and 10 mM GSSG (Figure 4).

Structural Differences between Observed Glutaredoxin States. The three observed states of glutaredoxin in equilibrium with glutathione are (i) the reduced enzyme, (ii) the glutathionylated enzyme, in which glutathione is covalently attached to $hGRX^{4CS}$ through a disulfide bond to Cys23, and (iii) the complex between reduced $hGRX^{4CS}$ and GSH. The structures of reduced wild type hGRX and glutathionylated $hGRX^{4CS}$ are

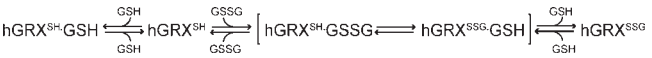

Figure 4. Schematic overview of different states of glutaredoxin (hGRX) during the reaction with glutathione. Three different states are experimentally observed corresponding to the reduced enzyme ($hGRX^{SH}$), the glutathionylated enzyme ($hGRX^{SSG}$), and the GSH bound reduced enzyme ($hGRX^{SH}\cdot GSH$). The reaction between $hGRX^{SH}$ and oxidized glutathione (GSSG) must proceed though the putative complexes [$hGRX^{SH}\cdot GSSG$] and [$hGRX^{SSG}\cdot GSH$] although these are not observed experimentally.

very similar with an overall rmsd between the mean structures of 0.96 Å.[21,25] Calculation of the mean displacement of each C^α atom relative to all other C^α atoms between the two structures revealed that the largest differences are in the loop regions and the C-terminal end (Figure 5A,B). Comparing the ^{15}N chemical shifts of reduced $hGRX^{4CS}$ with the ^{15}N chemical shifts of glutathionylated $hGRX^{4CS}$ shows significant differences (Figure 5C,D). The largest were for Lys20, Cys23, Arg28, Ala29, Ala67, Arg68, Thr69, Val70, Ile80, and Ser83. Panels A and C in Figure 5 show that chemical shift differences around residues Cys23 and Thr69 correspond to the largest structural changes of up to 1.4 Å while the chemical shift change for Ser83 is associated with a mean backbone displacement of only 0.5 Å. Chemical shift data for Asn52 are not available, as the resonance was missing from the spectra. From the titration of reduced $hGRX^{4CS}$ with GSH, structural information about the GSH binding site was obtained. The largest differences were for Lys20, Thr22, and Val70. The change in chemical shift of Cys23 is, not surprisingly, much less than when glutathione is covalently bound. The changes in the chemical shifts of the other residues are also less pronounced. Still, the pattern shows that GSH binds to reduced $hGRX^{4CS}$ in the binding site of covalently attached glutathione. The smaller chemical shift changes for the binding of GSH also indicate that the mere presence of the ligand is insufficient to account for all changes in chemical shifts observed between free and glutathionylated $hGRX^{4CS}$.

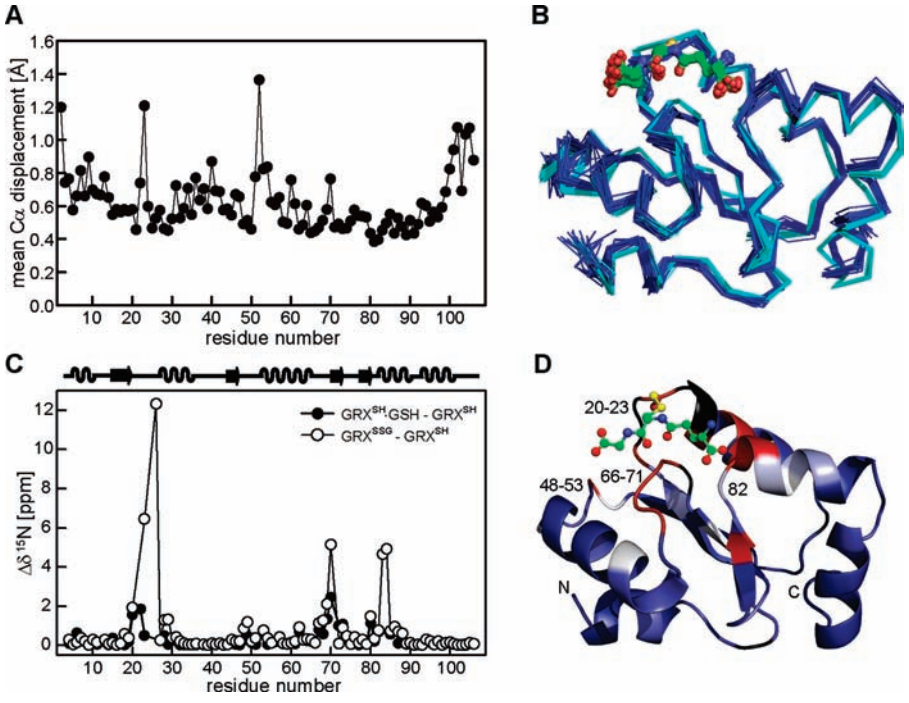

Figure 5. ^{15}N chemical shift differences between glutaredoxin states. (A) Mean C^α displacement calculated as the mean of residue-by-residue $C^\alpha-C^\alpha$ position difference between the lowest energy structure of glutathionylated $hGRX^{4CS}$ and of reduced hGRX. (B) Alignment of the 20 NMR structures of lowest energy of glutathionylated $hGRX^{4CS}$ (cyan) (PDB id: 1B4Q) with the 20 lowest energy structures of reduced wild type hGRX (dark blue) (PDB id: 1JHB), with a root-mean-square deviation of 0.96 Å from alignment with Pymol (DeLano Scientific). (C) Chemical shift differences between reduced glutaredoxin (1 mM ^{15}N-$hGRX^{4CS}$, 5 mM DTT) and glutathionylated glutaredoxin (^{15}N-$hGRX^{4CS}$) and between reduced glutaredoxin (^{15}N-$hGRX^{4CS}$, 5 mM DTT) and the complex of reduced glutaredoxin with GSH (^{13}C,^{15}N-$hGRX^{4CS}$, 5 mM DTT, 128 mM GSH) are shown. All spectra were recorded at 25 °C, pH 7.0. Differences are observable in the same areas although largest when glutathione is covalently attached to Cys23 through a disulfide bond. The secondary structure of glutaredoxin is displayed on top. (D) Cartoon representation of glutathionylated glutaredoxin with glutathione displayed in sticks (PDB id: 1B4Q). The structure is colored according to the chemical shift difference between reduced $hGRX^{4CS}$ and glutathionylated $hGRX^{4CS}$ with a color gradient running from dark blue over white to dark red with 29 colors with dark blue corresponding to less than 0.005 ppm difference and dark red corresponding to more than 1 ppm difference. Black denotes proline residues and residues not assigned in at least one of the states.

dx.doi.org/10.1021/ja1096539 |J. Am. Chem. Soc. 2011, 133, 3034–3042

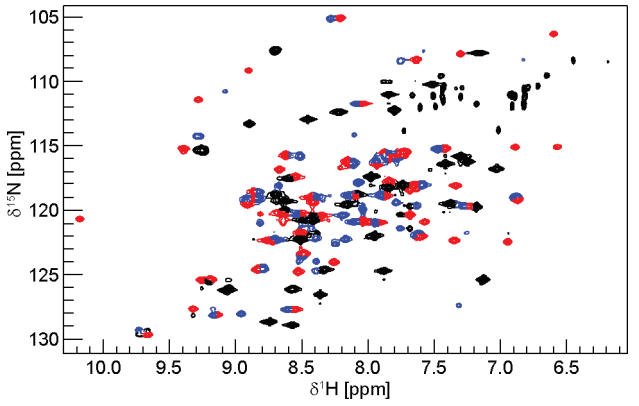

Figure 6. ^{15}N,^{1}H-HSQC glutathione reaction-sample used in the CPMG experiment. Peaks from the glutathionylated state are red and from the reduced state blue. Peaks with spectral overlap and unassigned peaks are black. No relaxation dispersion enhancement was found for any of the unassigned peaks. The experiments were recorded at 25 °C, pH 7.0, on 1 mM ^{15}N-hGRX^{4CS}. The reaction sample contained 22 μM GSSG and 560 μM GSH.

Microsecond−Millisecond Conformational Fluctuations in Glutaredoxin. Backbone motions in glutaredoxin during catalysis and in the two resting states were investigated by CPMG ^{15}N spin relaxation dispersion experiments. To measure dynamics in hGRX^{4CS} related to catalysis, the concentrations of GSH and GSSG were adjusted to reach slow exchange between the reduced and glutathionylated enzyme on the NMR time scale. Therefore, cross-peaks originating from backbone amides in both exchanging states are visible in the spectra (Figure 6), and the relaxation dispersions become independent of field strength.[32] In the resting states, no relaxation dispersions are observed, demonstrating that the backbone of the enzyme displays no significant dynamics on the millisecond time scale (Figure 7). The reaction sample was set up with 1 mM hGRX^{4CS}, 320 μM free GSH, and 140 μM free GSSG by dialysis. These concentrations correspond to a population of about ten percent reduced hGRX^{4CS} and k_{ex} of 190 s^{-1} as gauged from eqs 6 and 11. In the heteronuclear single quantum coherence (HSQC) spectrum of the sample, cross-peaks from a number of residues were identified as originating from either the glutathionylated state or the reduced state by comparison with spectra of the free forms (Figure 6). The chemical shift differences ($\Delta\omega$) obtained by fitting a two-state exchange model (eq 12) to the relaxation dispersion data correlate with the chemical shift difference between the two resting states ($\Delta\delta$) (Figure 7A and Table S1, Supporting Information) and reveal that no intermediate states are needed to explain the experimental data. At the chosen conditions the hGRX^{SH}·GSH off-path state was populated to less than one percent, and therefore not detectable in the experiment. Significant dispersions in ^{15}N-backbone R_2 relaxation rates were found for 23 residues of which nine have the N^{H} atoms within 6 Å of bound glutathione. The direct chemical effect from electrons in the substrate must be large on these residues (Figures 7and 8; Figure S1 and Table S2, Supporting Information). The largest dispersions were seen for Val70 and Cys23, as expected from the chemical shift differences between hGRX^{SH} and hGRX^{SSG} (Figures 5 and 7). Dispersions were also detected for Tyr25, Ser26, and Ser83, but the analysis is unreliable since the effect of the exchange process is not fully

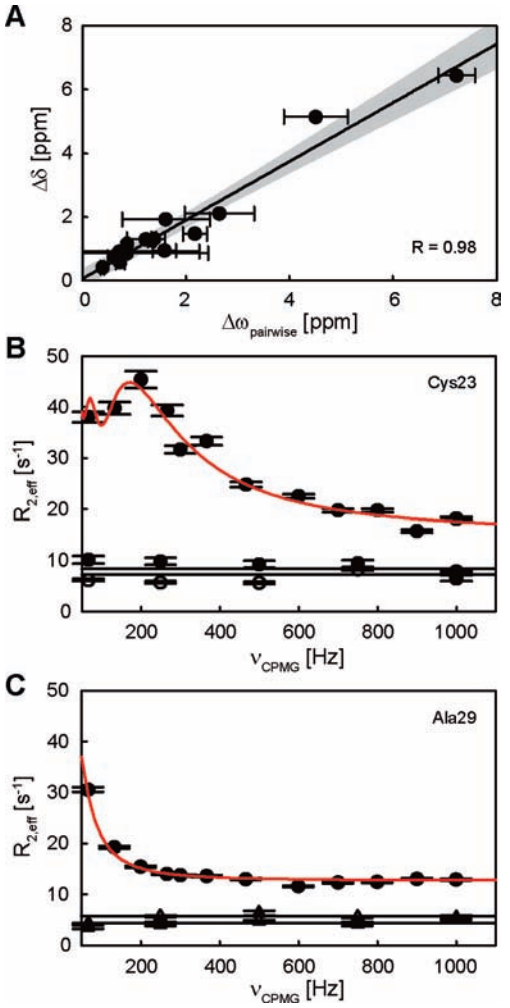

Figure 7. Microsecond−millisecond conformational motions in glutaredoxin. (A) Chemical shift correlation of $\Delta\omega$ from pairwise fits of R_2 dispersion data out of the glutathionylated state and out of the reduced state with the observed chemical shift difference between the two resting states ($\Delta\delta$). The linear fit with 95% confidence intervals is shown. (B) R_2 dispersion of catalytic active Cys23 during reaction (filled circles) and in the two resting states: reduced (open triangles), glutathionylated (filled triangles). The red curve is a global fit of eq 12 to the reaction data. Data from the resting states are fitted to a constant. Errors are estimated from the signal-to-noise level in the spectra. (C) R_2 dispersion of Ala29 during reaction and in the two resting states. Symbols and curves as for B. The experiments were recorded at 25 °C, pH 7.0, on 1 mM ^{15}N-hGRX^{4CS}. The reaction sample contained 22 μM GSSG and 560 μM GSH. The reduced sample contained 5 mM DTT.

suppressed even at the highest CPMG pulsing frequency. This behavior results mainly from the large chemical shift changes of these residues. That these residues located in the active site may experience additional dynamics cannot be ruled out. Asp59 is not included, as it is in intermediate exchange, and the parameters are not well-defined by the experiment.

A global fit of k_a^{ox} and k_a^{red} (eq 12) to the dispersion data gives k_{ex} of 51.2 ± 1.2 s^{-1}, and a population of hGRX^{SH} of 47% (Table S2). This result corresponds to [GSH] = 560 μM and [GSSG] = 22 μM and shows that an undesired shift in the equilibrium had occurred during sample preparation. At the low glutathione concentrations used in the experiment, accurate determination of the concentrations directly in the sample are not possible.

dx.doi.org/10.1021/ja1096539 |J. Am. Chem. Soc. 2011, 133, 3034–3042

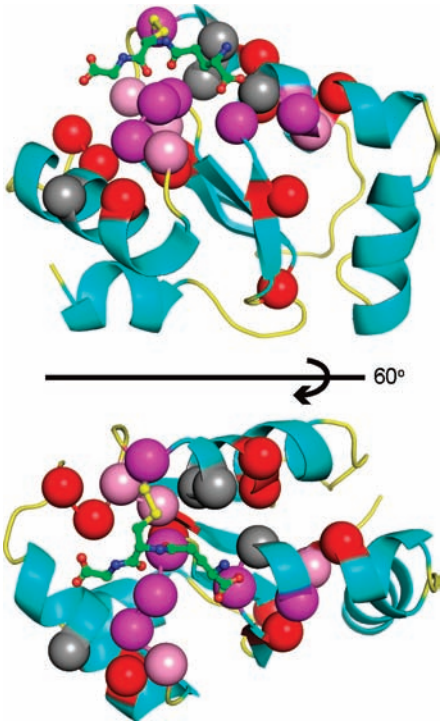

Figure 8. Residues with enhanced relaxation dispersion rates. Residues showing enhanced amide R_2 dispersion during reaction are displayed with backbone C^{α} atoms in the space-filling model. Residues with N^H within 6 Å from atoms in bound glutathione are magenta, residues with N^H more than 6 Å away but less than 8 Å are pink, and the remainder are red. Red, pink, and magenta residues are included in the global fit of k_{ex}. Tyr25, Ser26, Asp59, and Ser83 are colored gray, as they are not included in the global fit. The displayed structure is the lowest energy structure of glutathionylated $hGRX^{4CS}$ (PDB id: 1B4Q) with glutathione in balls and sticks.

[GSH] was estimated to 300−650 μM by HPLC whereas [GSSG] was below 100 μM, which is consistent with the glutathione concentrations calculated from the kinetics. The shift in the equilibrium does not influence the conclusions drawn from the data. Precautions were taken to avoid oxygen in the sample, as oxidation may result in drifting of the glutathione concentrations. No intensity differences, however, were observed in HSQC spectra before and after the NMR experiment, demonstrating that the glutathione concentrations were constant during the experiment.

Binding Dynamics of Glutaredoxin. Because motions were not detected in the resting states of the enzyme, the observed motions could be linked to transition state barrier crossing or to binding of substrates. The observation that GSH binds to the reduced enzyme in the binding site of covalently bound glutathione permitted discrimination between these two options. That residues showing exchange during catalysis are the same as those that change their chemical shifts when $hGRX^{SH}$ becomes glutathionylated and when GSH is added to $hGRX^{SH}$ suggest that only one-half of GSSG makes significant interactions with the enzyme. Binding of GSH and GSSG should occur, therefore, with comparable rates. If binding is limiting, we will consequently expect to observe comparable rates for GSH binding and turnover. If on the other hand transition state barrier crossing is limiting, GSH binding should be faster than turnover.

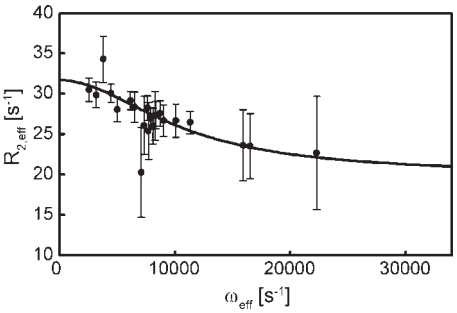

Figure 9. Conformational fluctuations of glutaredoxin upon binding of GSH. Relaxation dispersion profile of $R_{2,eff} = R_2 + R_{ex}$ (extracted from eq 13) for Val70 as function of the effective field strength. The solid line represents a fit of the relaxation dispersion data to eq 13 with k_{ex} as a global parameter for the three residues that show exchange (Lys20, Thr22, and Val70). ϕ_{ex} were fixed to the calculated values based on the GSH titration data. Standard errors on $R_{2,eff}$ are propagated from eq 13. The experiment was performed on a sample of 1 mM ^{15}N-$hGRX^{4CS}$ with 1.7 mM GSH, 5 mM DTT, pH 7.0, at 25 °C.

Dynamics in the backbone associated with binding of GSH to the reduced enzyme were investigated by off-resonance rotating-frame ($R_1\rho$), relaxation dispersion measurements. Using the determined value of K_2, a GSH concentration of 1.7 mM was chosen to populate the minor state ($hGRX^{4CS}$·GSH) to 10%. Small, yet significant, relaxation dispersions were observable for the three amides with the largest chemical shift differences (Figure 9). As expected from the GSH-induced chemical shift changes on $hGRX^{SH}$ (Figure 5C), no significant relaxation dispersion was detected for Cys23. A global fit of k_{ex} (eq 13) to the dispersion curves of Lys20, Thr22, and Val70 yields k_{ex} of 10510 ± 720 s^{-1}. Using this value of k_{ex} in combination with K_2 gives the rate constants k_2 of $(0.61 \pm 0.04) \times 10^6$ M^{-1} s^{-1} and k_{-2} of $(9.5 \pm 0.6) \times 10^3$ s^{-1}. The on-rate constant, k_2, is within a factor of 2 similar to the forward rate constant k_1, for GSSG turnover. Binding of GSH in the active site thus results in dynamics in $hGRX^{4CS}$ similar to that observed during catalysis.

DISCUSSION

Conformational Fluctuations Are Linked to Binding. The analysis of slow microsecond−millisecond backbone conformational fluctuations in $hGRX^{4CS}$ during catalysis of glutathione interchange shows that k_{ex} calculated from a global fit of the R_2 dispersion curves agrees with the catalytic turnover rate. The processes detected by the enzyme and by the substrate must, therefore, be limited by the same event. The correlation of the chemical shift difference between the two exchanging states and that between reduced and glutathionylated $hGRX^{4CS}$ reveals that the two exchanging states correspond to the reduced and glutathionylated states of the enzyme. This is characteristic for a two-state process. These data alone do not reveal whether the kinetics of the fluctuations is limited by binding alone or whether crossing of the catalytic energy barrier to product formation also contributes.

The finding that GSH binds to reduced $hGRX^{4CS}$ forming an off-pathway complex allowed testing if the conformational fluctuations in glutaredoxin are directly induced by binding. Analysis of microsecond−millisecond fluctuations in reduced $hGRX^{4CS}$ during binding of GSH revealed motions similar to those observed for $hGRX^{4CS}$ during catalysis. The rate

dx.doi.org/10.1021/ja1096539 |J. Am. Chem. Soc. 2011, 133, 3034–3042

constant for binding of GSH (k_2) is highly similar to k_1 differing only by a factor of 2. The similar kinetics of the two processes suggest that the conformational changes in hGRX^{4CS} observed during catalysis are linked directly to binding of glutathione and that no intermediates populate to an extent that influences the rate of product formation. In contrast, the rate of dissociation of hGRX^{4CS}·GSH (k_{-2} = 9.5 × 10^3 s^{-1}) is much faster than the concentration-dependent rate of the bimolecular reaction of deglutathionylation of hGRX^{4CS} (Scheme 1), which takes place at a rate of k_{-1} × [GSH] (for [GSH] = 320 μM the rate is 14 s^{-1}).

The experiments probe changes in the magnetic environment although contributions from conformational fluctuations cannot be distinguished from the sole effect of ligand presence. Therefore, the observed dispersion on residues close to the ligand may contain contributions from both. Nine of the twenty-three residues showing exchange during catalysis have N^H atoms within 6 Å from bound glutathione whose chemical shifts will be highly dependent on the change in electronic environment from binding alone (Figure 8). Electrostatic effects may reach further than 6 Å but will be small and difficult to predict. Ten of the twenty-three residues (Phe18, Arg28, Ala29, Ile48, Thr49, Asp59, Gln62, Gly76, Gly80, and Val87) have N^H atoms more than 8 Å away from the ligand. Enhanced dispersions on these residues likely reflect conformational motions. All together the present results show that microsecond−millisecond conformational fluctuations are present in hGRX^{4CS} only during catalysis of the glutathione interchange and when the reduced enzyme binds reduced glutathione. These observations infer that the observed motions, and thus the change in conformation between the free and bound forms of hGRX^{4CS}, are a direct result of binding glutathione and that binding occurs through an induced fit mechanism.

Lack of Intrinsic Microsecond−Millisecond Backbone Dynamics in Glutaredoxin. The finding that microsecond−millisecond conformational fluctuations are not detectable in the resting states of hGRX^{4CS} distinguishes hGRX^{4CS} from many other investigated enzymes.[10] NMR dispersion data yield neither information about amplitude nor direction of an observed fluctuation. This information can be obtained by coupling chemical shift of interchanging states to structural data. Intrinsic microsecond−millisecond dynamics in adenylate kinase is associated with large loop movements whereas movements in RNase A and dihydrofolate reductase are of smaller amplitude.[8,13,33] Collectively these fluctuations allow for substrates and products to access the active site. In all three enzymes, product release is rate-limiting for catalysis. The active site of hGRX^{4CS} is not protected by a loop, and the absence of resting state backbone fluctuations reflects the direct access to the active site.

A consequence of missing dynamics in the resting states comparable to the turnover rate is that hGRX^{4CS} cannot follow a mechanism where catalysis is controlled by conformer selection in substrate binding or product release. The latter is supported by the failure to saturate hGRX with substrate concentrations up to 50 mM GSH and 10 mM GSSG. If the chemical shift differences associated with fluctuations between the two states are very small in the absence of ligand, however, they may not be probed by the CPMG experiment. Likewise, the population of a higher energy state may also be so low that it is nonprobable by the NMR experiment. The involvement of such a high energy binding competent state in hGRX^{4CS} can be excluded, as substrate saturation was not observed.

Fluctuations between different conformers of hGRX may occur on even faster time-scales than probed here. Indeed, the order parameters for reduced *E. coli* GRX1 are lower than those for the oxidized state, implying that the fast (picosecond−nanosecond) dynamics has a higher amplitude in the reduced state than in the oxidized state.[34] This fast dynamics cannot be limiting for substrate binding and catalytic turnover, however. A fast pre-equilibrium between a major state and a binding-competent minor state would result in lowering the effective concentration of the active enzyme, implying that the enzyme had to be more efficient than if there were no pre-equilibrium.

Induced fit and conformational selection are two extreme models for ligand binding. Some elements of conformer selection likely occur in binding reactions that appear to follow an induced fit model (and vise versa) even if they are not observed.[1,16,19] Our results only describe backbone fluctuations. Specific side-chain conformations may still be selected as found for FKBP12 where backbone and side-chain microsecond−millisecond fluctuations are independent in a complex with the transition state analogue FK506.[35] It remains to be investigated whether the latter is also the case for hGRX^{4CS}, allowing for an element of side-chain conformer selection in addition to the predominating induced fit mechanism for substrate binding.

Catalysis by Glutaredoxin. In conclusion, the lack of resting state conformational fluctuations combined with the finding that k_{ex} obtained from the relaxation dispersion data corresponds to k_{ex} of the reaction suggests that the turnover rate of glutaredoxin is controlled by formation of a productive encounter complex between enzyme and substrate, and that the conformational changes subsequently occur by an induced fit mechanism. The latter cannot be rate-limiting, as no indication of substrate saturations were observed in accord with previous kinetic analysis showing that saturation was impossible.[22] The identified microscopic rate constants are consistent with earlier interpretations identifying the reaction between glutathionylated glutaredoxin and GSH as the rate-limiting step in the catalytic cycle of hGRX^{4CS}.[22] The present data fit a two-state model in which population of an encounter complex is not detectable, reflecting high commitment to catalysis. Our analysis of hGRX^{4CS} catalysis of the glutathione interchange reaction illustrates that conformational dynamics need not control the catalytic mechanism of an enzyme and that hGRX^{4CS} functions by providing optimal conditions for thiol−disulfide exchange. A general unifying model to explain the connection between conformational dynamics in enzymes and catalysis will have to account for different rate-limiting events in different enzymes.[1,16,19]

■ ASSOCIATED CONTENT

Supporting Information. Figure S1: R_2 relaxation dispersion plots of residues showing enhanced dispersion during reaction. Table S1: Fitting parameters for pairwise fit of dispersion data. Table S2: Fitting parameters from global fit of the relaxation dispersion data. This material is available free of charge via the Internet at http://pubs.acs.org.

■ AUTHOR INFORMATION

Corresponding Author
kaare.teilum@bio.ku.dk

Present Addresses
[†]Chemistry Department, Institute for Biophysical Chemistry, TU München, Lichtenbergstrasse 4, D-85748 Garching, Germany.

■ ACKNOWLEDGMENT

This work was supported by the Danish Research Agency for Nature and Universe grant number 272-06-0251 (K.T.). K.S.J. received a stipend from Faculty of Science, University of Copenhagen. Dr. Bent W. Sigurskjold is thanked for an introduction to the isothermal titration calorimetry setup. We thank Penny von Wettstein-Knowles for critically reviewing the manuscript of this paper.

■ REFERENCES

(1) Teilum, K.; Olsen, J. G.; Kragelund, B. B. *Cell. Mol. Life Sci.* **2009**, *66*, 2231–2247.
(2) Wolf-Watz, M.; Thai, V.; Henzler-Wildman, K.; Hadjipavlou, G.; Eisenmesser, E. Z.; Kern, D. *Nat. Struct. Mol. Biol.* **2004**, *11*, 945–949.
(3) Doucet, N.; Watt, E. D.; Loria, J. P. *Biochemistry* **2009**, *48*, 7160–7168.
(4) Kovrigin, E. L.; Loria, J. P. *J. Am. Chem. Soc.* **2006**, *128*, 7724–7725.
(5) Schwartz, S. D.; Schramm, V. L. *Nat. Chem. Biol.* **2009**, *5*, 551–558.
(6) Kovrigin, E. L.; Loria, J. P. *Biochemistry* **2006**, *45*, 2636–2647.
(7) Boehr, D. D.; McElheny, D.; Dyson, H. J.; Wright, P. E. *Proc. Natl. Acad. Sci. U.S.A.* **2010**, *107*, 1373–1378.
(8) Boehr, D. D.; McElheny, D.; Dyson, H. J.; Wright, P. E. *Science* **2006**, *313*, 1638–1642.
(9) Palmer, A. G., III; Kroenke, C. D.; Loria, J. P. *Methods Enzymol.* **2001**, *339*, 204–238.
(10) Kern, D.; Eisenmesser, E. Z.; Wolf-Watz, M. *Methods Enzymol.* **2005**, *394*, 507–524.
(11) Eisenmesser, E. Z.; Millet, O.; Labeikovsky, W.; Korzhnev, D. M.; Wolf-Watz, M.; Bosco, D. A.; Skalicky, J. J.; Kay, L. E.; Kern, D. *Nature* **2005**, *438*, 117–121.
(12) Eisenmesser, E. Z.; Bosco, D. A.; Akke, M.; Kern, D. *Science* **2002**, *295*, 1520–1523.
(13) Henzler-Wildman, K. A.; Thai, V.; Lei, M.; Ott, M.; Wolf-Watz, M.; Fenn, T.; Pozharski, E.; Wilson, M. A.; Petsko, G. A.; Karplus, M.; Hubner, C. G.; Kern, D. *Nature* **2007**, *450*, 838–844.
(14) Henzler-Wildman, K. A.; Lei, M.; Thai, V.; Kerns, S. J.; Karplus, M.; Kern, D. *Nature* **2007**, *450*, 913–916.
(15) Labeikovsky, W.; Eisenmesser, E. Z.; Bosco, D. A.; Kern, D. *J. Mol. Biol.* **2007**, *367*, 1370–1381.
(16) Grunberg, R.; Leckner, J.; Nilges, M. *Structure* **2004**, *12*, 2125–2136.
(17) Koshland, D. E. *Proc. Natl. Acad. Sci. U.S.A* **1958**, *44*, 98–104.
(18) Boehr, D. D.; Nussinov, R.; Wright, P. E. *Nat. Chem. Biol.* **2009**, *5*, 789–796.
(19) Csermely, P.; Palotai, R.; Nussinov, R. *Trends Biochem. Sci.* **2010**, *35*, 539–546.
(20) Lillig, C. H.; Berndt, C.; Holmgren, A. *Biochim. Biophys. Acta* **2008**, *1780*, 1304–1317.
(21) Yang, Y.; Jao, S.; Nanduri, S.; Starke, D. W.; Mieyal, J. J.; Qin, J. *Biochemistry* **1998**, *37*, 17145–17156.
(22) Srinivasan, U.; Mieyal, P. A.; Mieyal, J. J. *Biochemistry* **1997**, *36*, 3199–3206.
(23) Jensen, K. S.; Hansen, R. E.; Winther, J. R. *Antioxid. Redox. Signal.* **2009**, *11*, 1047–1058.
(24) Delaglio, F.; Grzesiek, S.; Vuister, G. W.; Zhu, G.; Pfeifer, J.; Bax, A. *J. Biomol. NMR* **1995**, *6*, 277–293.
(25) Sun, C.; Holmgren, A.; Bushweller, J. H. *Protein Sci.* **1997**, *6*, 383–390.
(26) Robinson, G.; Kuchel, P. W.; Chapman, B. E.; Doddrell, D. M.; Irving, M. G. *J. Magn. Reson.* **1985**, *63*, 314–319.
(27) Loria, J. P.; Rance, M.; Palmer, A. G. *J. Am. Chem. Soc.* **1999**, *121*, 2331–2332.
(28) Tollinger, M.; Skrynnikov, N. R.; Mulder, F. A.; Forman-Kay, J. D.; Kay, L. E. *J. Am. Chem. Soc.* **2001**, *123*, 11341–11352.
(29) Iversen, R.; Andersen, P. A.; Jensen, K. S.; Winther, J. R.; Sigurskjold, B. W. *Biochemistry* **2010**, *49*, 810–820.
(30) Led, J. J.; Gesmar, H.; Abildgaard, F. *Methods Enzymol.* **1989**, *176*, 311–329.
(31) Rabenstein, D. L.; Millis, K. K. *Biochim. Biophys. Acta* **1995**, *1249*, 29–36.
(32) Millet, O.; Loria, J. P.; Kroenke, C. D.; Pons, M.; Palmer, A. G. *J. Am. Chem. Soc.* **2000**, *122*, 2867–2877.
(33) Beach, H.; Cole, R.; Gill, M. L.; Loria, J. P. *J. Am. Chem. Soc.* **2005**, *127*, 9167–9176.
(34) Kelley, J. J., III; Caputo, T. M.; Eaton, S. F.; Laue, T. M.; Bushweller, J. H. *Biochemistry* **1997**, *36*, 5029–5044.
(35) Brath, U.; Akke, M. *J. Mol. Biol.* **2009**, *387*, 233–244.